Supporting Information

Tuning of Multi-instabilities in Organic Alloy, $[(EDO\text{-}TTF)_{1-x}(MeEDO\text{-}TTF)_x]_2PF_6$

Tsuyoshi Murata, Xiangfeng Shao, Yoshiaki Nakano, Hideki Yamochi, Mikio Uruichi, Kyuya Yakushi, Gunzi Saito, and Koichiro Tanaka

Figure S1. Photographs of crystals of $(Me_xEDO\text{-}TTF)_2PF_6$, (a) batch 4 ($x$ = 0.13–0.15), (b) batch 9 (x = 0.52–0.55), (c) batch 10 (including both $(EDO\text{-}TTF)_2PF_6$ type (x = 0.51–0.55) and $(MeEDO\text{-}TTF)_2PF_6$ type (x = 0.91–0.94) alloys), and (d) batch 11 (x = 0.92–0.94). The crystals were placed on the graph paper with a grid size of 1 × 1 mm^2 squares.

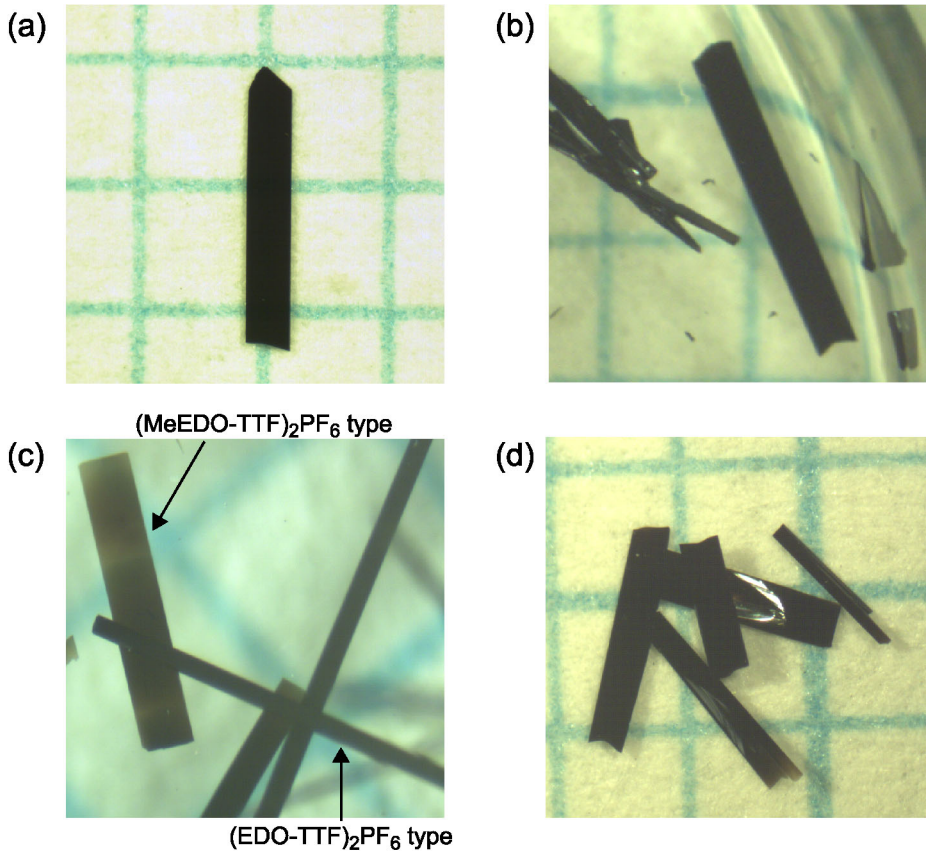

Table S1. Crystallographic data of $(Me_xEDO\text{-}TTF)_2PF_6$ (x = 0.22 (batch 5), 0.37 (batch 6, the sample of X-ray analysis is not same as that of conductivity measurement), and 0.44 (batch 7) measured at room temperature.

	$x = 0.22$	$x = 0.37$	$x = 0.44$
formula	$C_{16.44}H_{12.88}F_6O_4PS_8$	$C_{16.74}H_{13.48}F_6O_4PS_8$	$C_{16.88}H_{13.76}F_6O_4PS_8$
formula weight	675.88	680.09	682.05
crystal system	triclinic	triclinic	triclinic
space group	$P\bar{1}$	$P\bar{1}$	$P\bar{1}$
a, Å	7.241(2)	7.237(3)	7.271(3)
b, Å	7.355(2)	7.376(2)	7.372(3)
c, Å	12.100(3)	12.128(5)	12.219(5)
α, º	93.74(2)	93.88(3)	93.80(3)
β, º	75.45(2)	75.44(2)	75.47(3)
γ, º	96.88(1)	96.92(2)	96.70(2)
V, Å^3	618.8(3)	621.5(4)	629.2(4)
Z	1	1	1
d_{calc}, g cm^{-3}	1.814	1.817	1.800
μ(Mo Kα), cm^{-1}	0.857	0.854	0.844
no. of unique refln.	2140	2019	2009
no. of used refln.	1251	979	846
no. of params	188	194	194
R_1 ($I > 2.0\sigma(I)$)	0.0919	0.0716	0.0824
wR2 (all data)	0.2843	0.2562	0.2960
GOF	1.011	1.047	0.909

Table S2. Crystallographic data of $(Me_xEDO\text{-}TTF)_2PF_6$ (x = 0.03 (batch 2)) at 300–260 K.

	300 K	285 K	270 K	260 K
formula	$C_{16.06}H_{12.12}F_6O_4PS_8$	$C_{16.06}H_{12.12}F_6O_4PS_8$	$C_{16.06}H_{12.12}F_6O_4PS_8$	$C_{16.06}H_{12.12}F_6O_4PS_8$
formula weight	670.55	670.55	670.55	670.55
crystal system	triclinic	triclinic	triclinic	triclinic
space group	$P\bar{1}$	$P\bar{1}$	$P\bar{1}$	$P\bar{1}$
a, Å	7.203(1)	7.199(0.9)	7.197(1)	7.194(2)
b, Å	7.349(0.8)	7.336(0.8)	7.324(0.9)	7.319(1)
c, Å	11.965(2)	11.959(2)	11.952(2)	11.932(3)
α, º	93.495(8)	93.433(7)	93.346(9)	93.24(1)
β, º	75.196(7)	75.131(6)	75.079(7)	75.10(1)
γ, º	97.368(8)	97.349(7)	97.358(8)	97.38(1)
V, Å^3	607.0(2)	605.2(1)	603.5(2)	601.9(2)
Z	1	1	1	1
d_{calc}, g cm^{-3}	1.834	1.840	1.845	1.850
μ(Mo Kα), cm^{-1}	0.873	0.875	0.878	0.880
no. of unique refln.	2176	2167	2173	2107
no. of used refln.	1585	1608	1638	1561
no. of params	188	188	188	188
R_1 ($I > 2.0\sigma(I)$)	0.0542	0.0544	0.0571	0.0607
w$R2$ (all data)	0.1635	0.1641	0.1684	0.1833
GOF	1.092	1.107	1.115	1.082

Table S3. Crystallographic data of $(Me_xEDO\text{-}TTF)_2PF_6$ (x = 0.03 (batch 2)) at 250–100 K.

	250 K	240 K	200 K	150 K	100 K
formula	$C_{16.06}H_{12.12}F_6O_4PS_8$	$C_{16.06}H_{12.12}F_6O_4PS_8$	$C_{16.06}H_{12.12}F_6O_4PS_8$	$C_{16.06}H_{12.12}F_6O_4PS_8$	$C_{16.06}H_{12.12}F_6O_4PS_8$
formula weight	670.55	670.55	670.55	670.55	670.55
crystal system	triclinic	triclinic	triclinic	triclinic	triclinic
space group	$P\bar{1}$	$P\bar{1}$	$P\bar{1}$	$P\bar{1}$	$P\bar{1}$
a, Å	9.753(6)	9.765(5)	9.778(4)	9.760(3)	9.736(3)
b, Å	10.950(4)	10.969(3)	11.030(2)	11.083(2)	11.087(2)
c, Å	11.442(6)	11.415(6)	11.319(4)	11.203(3)	11.127(3)
α, º	101.81(3)	101.80(3)	101.67(2)	101.66(2)	101.65(2)
β, º	99.24(3)	99.37(2)	99.76(2)	100.22(1)	100.55(1)
γ, º	90.64(3)	90.40(3)	89.71(2)	88.72(2)	87.98(2)
V, Å^3	1179(1)	1179.9(9)	1177.7(6)	1167.9(5)	1156.5(5)
Z	2	2	2	2	2
d_{calc}, g cm^{-3}	1.888	1.887	1.891	1.907	1.926
μ(Mo Kα), cm^{-1}	0.897	0.898	0.900	0.907	0.916
no. of unique refln.	4039	3767	3985	3993	3978
no. of used refln.	2084	2219	2631	2890	3033
no. of params	316	316	316	316	316
R_1 ($I > 2.0\sigma(I)$)	0.0779	0.0699	0.0623	0.0471	0.0423
w$R2$ (all data)	0.2404	0.2092	0.1921	0.1339	0.1179
GOF	0.946	1.005	1.048	1.104	1.066

Table S4. Crystallographic data of $(Me_xEDO\text{-}TTF)_2PF_6$ (x = 0.05 (batch 3)) at 300–240 K.

	300 K	270 K	250 K	240 K
formula	$C_{16.10}H_{12.20}F_6O_4PS_8$	$C_{16.10}H_{12.20}F_6O_4PS_8$	$C_{16.10}H_{12.20}F_6O_4PS_8$	$C_{16.10}H_{12.20}F_6O_4PS_8$
formula weight	671.11	671.11	671.11	671.11
crystal system	triclinic	triclinic	triclinic	triclinic
space group	$P\bar{1}$	$P\bar{1}$	$P\bar{1}$	$P\bar{1}$
a, Å	7.205(0.7)	7.200(0.7)	7.198(0.6)	7.195(0.6)
b, Å	7.350(2)	7.326(2)	7.312(1)	7.302(1)
c, Å	11.982(2)	11.970(2)	11.962(2)	11.955(2)
α, º	93.527(9)	93.387(9)	93.288(8)	93.214(8)
β, º	75.232(9)	75.134(9)	75.048(8)	75.002(8)
γ, º	97.288(9)	97.30(1)	97.31(1)	97.305(9)
V, Å^3	608.3(2)	605.1(2)	603.1(2)	601.6(2)
Z	1	1	1	1
d_{calc}, g cm^{-3}	1.832	1.842	1.848	1.852
μ(Mo Kα), cm^{-1}	0.871	0.876	0.878	0.881
no. of unique refln.	2170	2152	2153	2144
no. of used refln.	1513	1569	1615	1612
no. of params	188	188	188	188
R_1 ($I > 2.0\sigma(I)$)	0.0541	0.0500	0.0478	0.0463
w$R2$ (all data)	0.1797	0.1622	0.1500	0.1442
GOF	1.076	1.090	1.072	1.069

Table S5. Crystallographic data of $(Me_xEDO\text{-}TTF)_2PF_6$ (x = 0.05 (batch 3)) at 230–100 K.

	230 K	200 K	150 K	100 K
formula	$C_{16.10}H_{12.20}F_6O_4PS_8$	$C_{16.10}H_{12.20}F_6O_4PS_8$	$C_{16.10}H_{12.20}F_6O_4PS_8$	$C_{16.10}H_{12.20}F_6O_4PS_8$
formula weight	671.11	671.11	671.11	671.11
crystal system	triclinic	triclinic	triclinic	triclinic
space group	$P\bar{1}$	$P\bar{1}$	$P\bar{1}$	$P\bar{1}$
a, Å	9.618(5)	9.805(3)	9.778(1)	9.759(1)
b, Å	10.918(6)	10.998(4)	11.065(2)	11.087(2)
c, Å	11.881(7)	11.487(4)	11.268(2)	11.162(2)
α, º	101.87(3)	101.77(2)	101.666(8)	101.643(7)
β, º	98.40(3)	99.69(2)	100.121(8)	100.520(8)
γ, º	90.83(3)	89.90(2)	88.786(8)	87.955(7)
V, Å^3	1207(1)	1194.7(7)	1175.2(3)	1163.0(3)
Z	2	2	2	2
d_{calc}, g cm^{-3}	1.847	1.866	1.896	1.916
μ(Mo Kα), cm^{-1}	0.878	0.887	0.902	0.911
no. of unique refln.	3692	4118	4150	4157
no. of used refln.	1578	2345	2805	3048
no. of params	326	316	316	316
R_1 ($I > 2.0\sigma(I)$)	0.1554	0.0749	0.0649	0.0462
w$R2$ (all data)	0.4968	0.2234	0.1941	0.1232
GOF	1.563	0.952	1.040	0.965

Table S6. Crystallographic data of $(Me_xEDO\text{-}TTF)_2PF_6$ (x = 0.13 (batch 4)) at 300–100 K.

	300 K	250 K	200 K	150 K	100 K
formula	$C_{16.26}H_{12.52}F_6O_4PS_8$	$C_{16.26}H_{12.52}F_6O_4PS_8$	$C_{16.26}H_{12.52}F_6O_4PS_8$	$C_{16.26}H_{12.52}F_6O_4PS_8$	$C_{16.26}H_{12.52}F_6O_4PS_8$
formula weight	673.35	673.35	673.35	673.35	673.35
crystal system	triclinic	triclinic	triclinic	triclinic	triclinic
space group	$P\bar{1}$	$P\bar{1}$	$P\bar{1}$	$P\bar{1}$	$P\bar{1}$
a, Å	7.211(0.6)	7.200(0.6)	7.192(0.6)	9.552(1)	9.517(1)
b, Å	7.354(1)	7.315(1)	7.277(0.7)	10.815(0.9)	10.806(1)
c, Å	12.022(2)	12.004(2)	11.981(1)	11.950(1)	11.928(2)
α, º	93.608(6)	93.380(6)	93.097(5)	101.836(6)	101.663(9)
β, º	75.377(7)	75.248(7)	75.109(7)	99.191(6)	99.631(7)
γ, º	97.105(8)	97.045(7)	97.041(6)	90.420(7)	90.246(8)
V, Å^3	611.8(1)	606.5(1)	601.3(1)	1191.7(2)	1183.5(3)
Z	1	1	1	2	2
d_{calc}, g cm^{-3}	1.828	1.844	1.860	1.877	1.890
μ(Mo Kα), cm^{-1}	0.866	0.874	0.881	0.889	0.896
no. of unique refln.	2160	2165	2153	4278	4269
no. of used refln.	1753	1763	1824	2590	2341
no. of params	188	188	188	335	316
R_1 ($I > 2.0\sigma(I)$)	0.0667	0.0646	0.0659	0.0825	0.0561
w$R2$ (all data)	0.1951	0.1814	0.1901	0.2937	0.2029
GOF	1.195	1.177	1.140	1.089	1.136

Table S7. Crystallographic data of $(Me_xEDO\text{-}TTF)_2PF_6$ (x = 0.48 (batch 8)) at 300 and 150 K.

	300 K	150 K
formula	$C_{16.96}H_{13.92}F_6O_4PS_8$	$C_{16.96}H_{13.92}F_6O_4PS_8$
formula weight	683.17	683.17
crystal system	triclinic	triclinic
space group	$P\bar{1}$	$P\bar{1}$
a, Å	7.286(1)	7.230(0.9)
b, Å	7.355(2)	7.261(1)
c, Å	12.258(3)	12.169(2)
α, º	93.91(1)	93.310(9)
β, º	75.50(1)	75.70(1)
γ, º	96.69(1)	96.155(8)
V, Å^3	631.1(2)	615.2(2)
Z	1	1
d_{calc}, g cm^{-3}	1.798	1.844
μ(Mo Kα), cm^{-1}	0.841	0.863
no. of unique refln.	2223	2199
no. of used refln.	1354	1572
no. of params	194	194
R_1 ($I > 2.0\sigma(I)$)	0.0750	0.0529
w$R2$ (all data)	0.2318	0.1635
GOF	1.001	1.080

Table S8. Crystallographic data of $(Me_xEDO\text{-}TTF)_2PF_6$ (x = 0.91 (batch 10) and 0.97 (batch 12)) measured at room temperature.

	x = 0.91	x = 0.97
formula	$C_{17.82}H_{15.64}F_6O_4PS_8$	$C_{17.94}H_{15.88}F_6O_4PS_8$
formula weight	695.23	696.92
crystal system	orthorhombic	orthorhombic
space group	*Cmcm*	*Cmcm*
a, Å	29.658(4)	29.672(3)
b, Å	12.608(2)	12.609(1)
c, Å	6.990(1)	6.992(0.4)
V, Å^3	2613.8(7)	2615.9(4)
Z	4	4
d_{calc}, g cm^{-3}	1.767	1.770
μ(Mo Kα), cm^{-1}	0.814	0.814
no. of unique refln.	1412	1392
no. of used refln.	779	1083
no. of params	121	121
R_1 ($I > 2.0\sigma(I)$)	0.0734	0.0789
wR2 (all data)	0.2552	0.2596
GOF	0.998	1.085

Table S9. Crystallographic data of $(Me_xEDO\text{-}TTF)_2PF_6$ (x = 0.94 (batch 11)) at 300–110 K.

	300 K	250 K	200 K	110 K
formula	$C_{17.88}H_{15.76}F_6O_4PS_8$	$C_{17.88}H_{15.76}F_6O_4PS_8$	$C_{17.88}H_{15.76}F_6O_4PS_8$	$C_{17.88}H_{15.76}F_6O_4PS_8$
formula weight	696.07	696.07	696.07	696.07
crystal system	orthorhombic	orthorhombic	orthorhombic	orthorhombic
space group	*Cmcm*	*Pbcn*	*Pbcn*	*Pbcn*
a, Å	29.662(3)	29.459(4)	29.396(3)	29.31(1)
b, Å	12.615(1)	12.607(2)	12.564(2)	12.572(7)
c, Å	6.994(0.5)	6.947(0.5)	6.906(0.5)	6.818(2)
V, Å^3	2617.1(4)	2580.0(6)	2550.6(5)	2513(2)
Z	4	4	4	4
d_{calc}, g cm^{-3}	1.767	1.792	1.813	1.840
μ(Mo Kα), cm^{-1}	0.813	0.825	0.834	0.847
no. of unique refln.	1447	2288	2254	2084
no. of used refln.	1072	1575	1664	880
no. of params	121	169	169	169
R_1 ($I > 2.0\sigma(I)$)	0.0696	0.0739	0.0501	0.0640
w$R2$ (all data)	0.2183	0.2062	0.1553	0.2030
GOF	1.074	1.009	1.088	0.893

Table S10. Intermolecular overlap integrals of $(Me_xEDO\text{-}TTF)_2PF_6$ ($x \leq 0.48$) and pristine $(EDO\text{-}TTF)_2PF_6$ ($x = 0$)[ref. 5] in the HT phase. The disordered methyl groups were replaced with hydrogen-atoms having sp^2 configuration of the bonding carbon atoms.

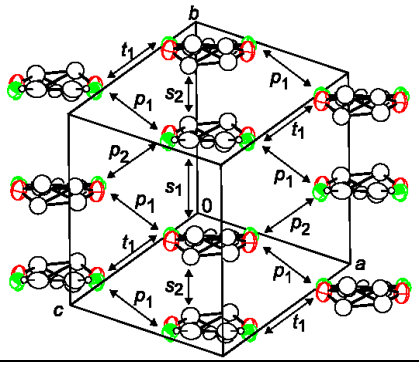

x	T	s_1	s_2	p_1	p_2	t_1
0[ref.5]	RT	27.4	27.3	–6.3	2.3	1.6
0.03	300 K	27.8	26.8	–6.3	2.2	1.5
	285 K	28.2	27.1	–6.4	2.3	1.4
	270 K	28.5	27.5	–6.4	2.3	1.4
	260 K	28.9	27.6	–6.5	2.4	1.4
0.05	300 K	27.6	26.9	–6.3	2.2	1.4
	270 K	28.5	27.4	–6.4	2.3	1.4
	250 K	28.8	27.9	–6.5	2.3	1.4
	240 K	29.1	28.1	–6.5	2.3	1.4
0.13	300 K	27.9	26.6	–6.3	2.2	1.2
	250 K	28.9	27.5	–6.5	2.2	1.2
	200 K	30.1	28.4	–6.6	2.3	1.2
0.22	RT	28.7	26.1	–6.0	2.2	1.0
0.37	RT	27.6	25.7	–5.9	2.3	1.0
0.44	RT	27.8	25.1	–5.7	2.2	0.9
0.48	300 K	28.9	25.4	–5.4	2.3	0.8
	150 K	31.5	27.5	–6.2	2.2	0.7

Table S11. Intermolecular overlap integrals of $(Me_xEDO\text{-}TTF)_2PF_6$ ($x \leq 0.13$) and pristine $(EDO\text{-}TTF)_2PF_6$ ($x = 0$)[ref. 5] in the LT phase. The disordered methyl groups were replaced with hydrogen-atoms having sp^2 configuration of the bonding carbon atoms.

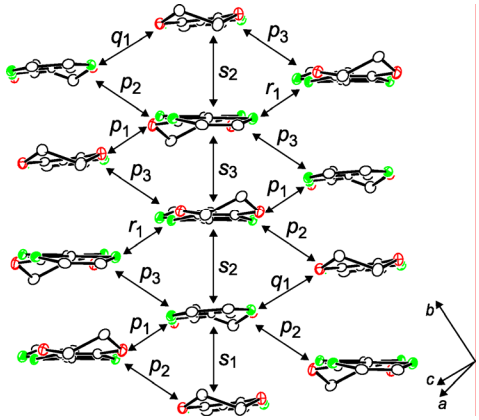

x	T	s_1	s_2	s_3	p_1	p_2	p_3	q_1	r_1
0[ref.5]	260 K	44.2	–23.0	13.0	–0.9	3.3	8.1	0.4	1.6
0.03	250 K	45.2	–24.6	13.6	–1.0	3.6	8.8	0.4	1.9
	240 K	45.5	–24.0	13.6	–1.0	3.4	8.8	0.4	1.7
	200 K	46.1	–23.6	13.4	–0.6	2.8	8.9	0.3	1.6
	150 K	46.7	–23.7	14.4	–0.3	2.4	8.6	0.2	1.6
	100 K	47.7	–24.6	15.6	–0.2	2.0	8.7	0.1	1.7
0.05	230 K	36.8	–28.0	20.5	–1.3	4.9	7.3	1.4	2.6
	200 K	45.6	–23.9	14.0	–0.8	3.2	8.4	0.4	1.6
	150 K	46.5	–23.9	14.5	–0.4	2.4	8.4	0.2	1.7
	100 K	47.4	–24.8	15.4	–0.2	2.0	8.5	0.1	1.6
0.13	150 K	32.3	–31.5	26.3	–1.2	6.5	7.1	2.2	2.4
	100 K	32.7	–32.5	26.7	–1.2	6.6	7.2	2.2	2.3

Table S12. Intermolecular overlap integrals of $(Me_xEDO\text{-}TTF)_2PF_6$ ($x \geq 0.91$) and pristine $(MeEDO\text{-}TTF)_2PF_6$ ($x = 1$).[ref.17] The disordered methyl group was included in the calculation.

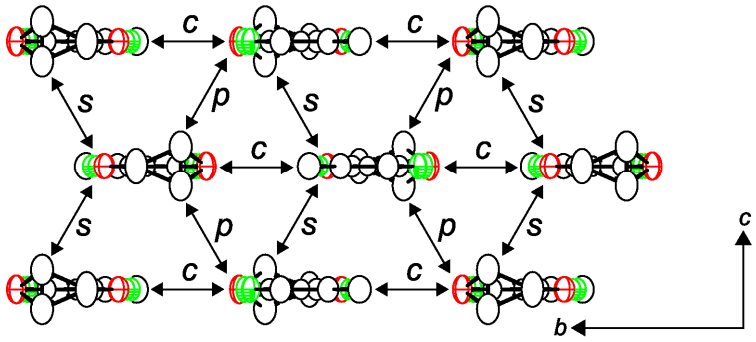

x	*T*	*c*	*p*	*s*
0.91	RT	9.8	8.9	–4.6
0.94	300 K	9.9	8.7	–4.9
	250 K	9.8	–9.1	4.9
	200 K	10.1	–9.3	5.0
	110 K	10.0	–9.7	4.9
0.97	RT	9.9	8.7	–5.0
1[ref.17]	302 K (HT phase)	–9.9	8.5	4.9
1[ref.17]	302 K (LT phase)	9.2	–8.5	4.9

Figure S2. Temperature dependence of resistivities measured for single crystals of EDO-TTF rich alloys (batches 1–8 and 10). All the data plotted were taken in the cooling processes. $T_{\sigma max}$ is the temperature at which resistivity shows a minimum. Probably due to crystal cracking or dull feature of the phase transition, resistivity of some crystals of $x \leq 0.13$ alloys showed a minimum at $T > T_c$. T_c was defined as the temperature at which abrupt increase or discontinuous behavior of resistivity was observed. σ_{RT} and $T_{\sigma max}$ strongly depended on crystal quality.

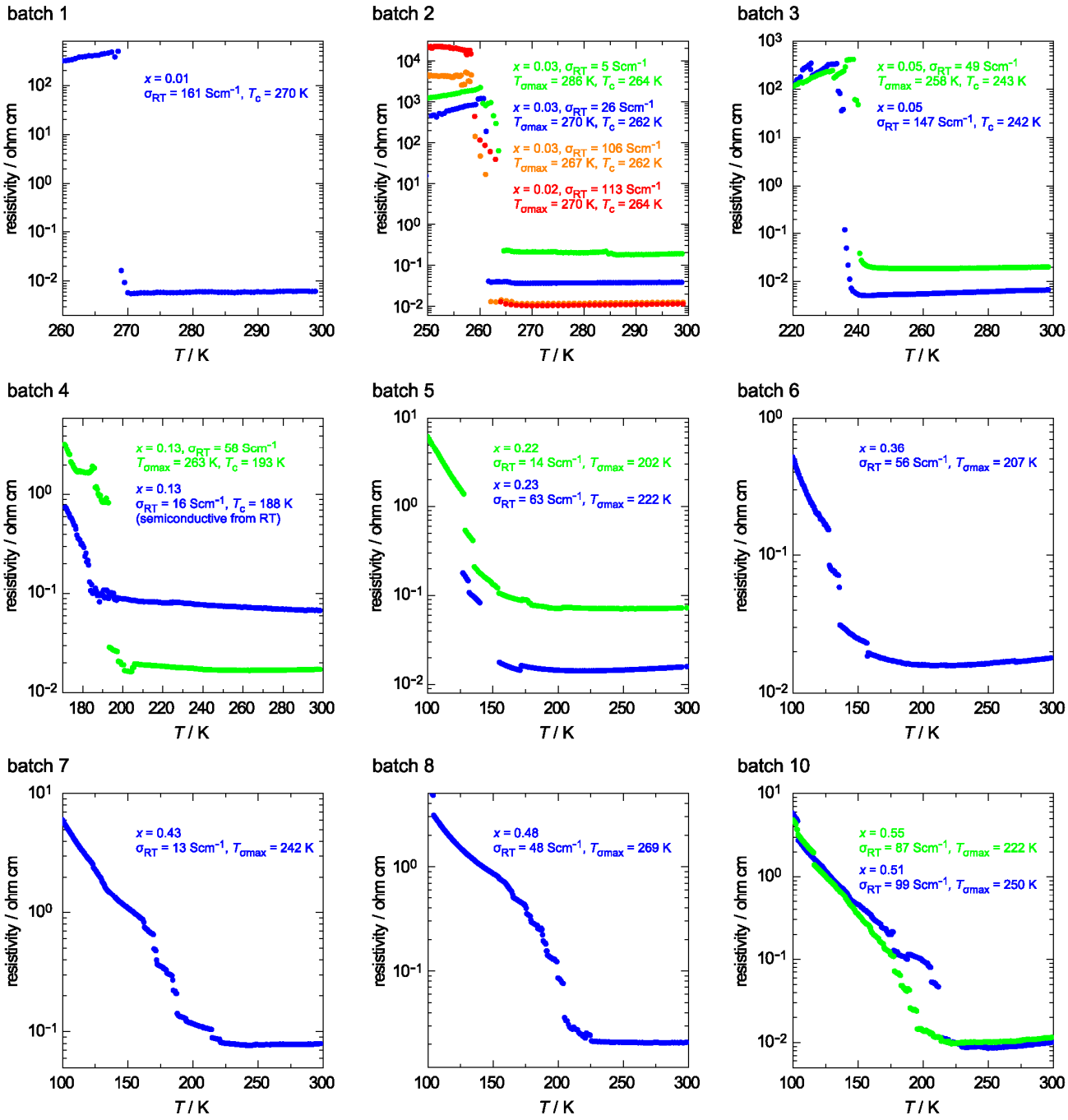

Figure S3. (a) Angular dependence of room temperature ESR spectra measured for a single crystal of $x = 0.53$ alloy (batch 9), applying magnetic field (H) within the bc plane. The black line shows the observed signal, which is reproduced as the sum of two Lorentzain lines (blue and green) within the noise range. (b) Angular dependence (H within bc plane) of g-factors of the two simulated Lorentzian lines. Colors of the plots correspond to those of the simulated lines in (a). (c) Temperature dependence of ESR spectra applying H along the b-axis.

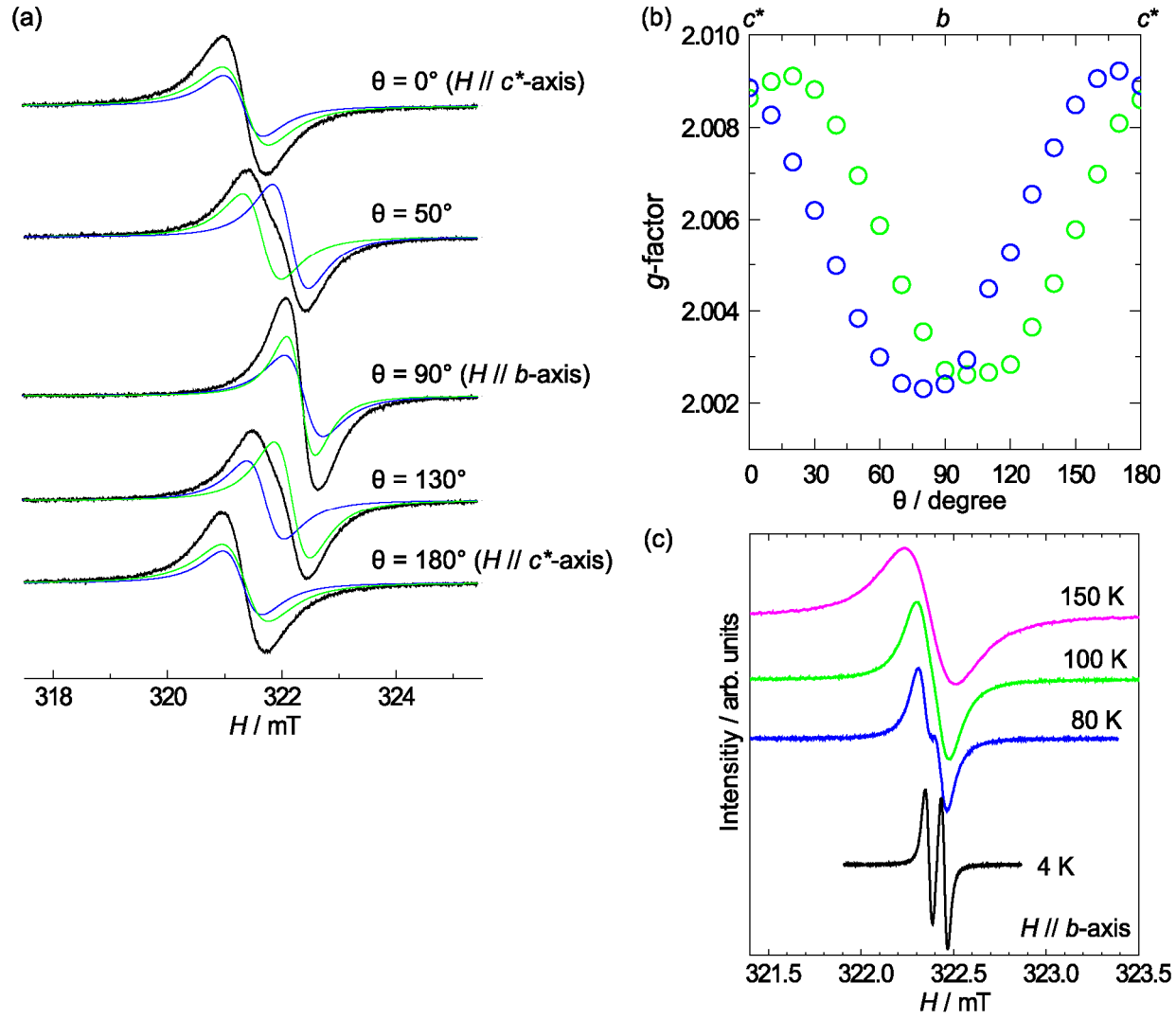

Figure S4. Temperature dependence of Raman spectra of x = 0.05 alloy (batch 3). Bands assignable as C=C stretching modes of EDO-TTF having 0, +0.5, and +1 charges are indicated by orange, green, and blue solid lines, respectively.

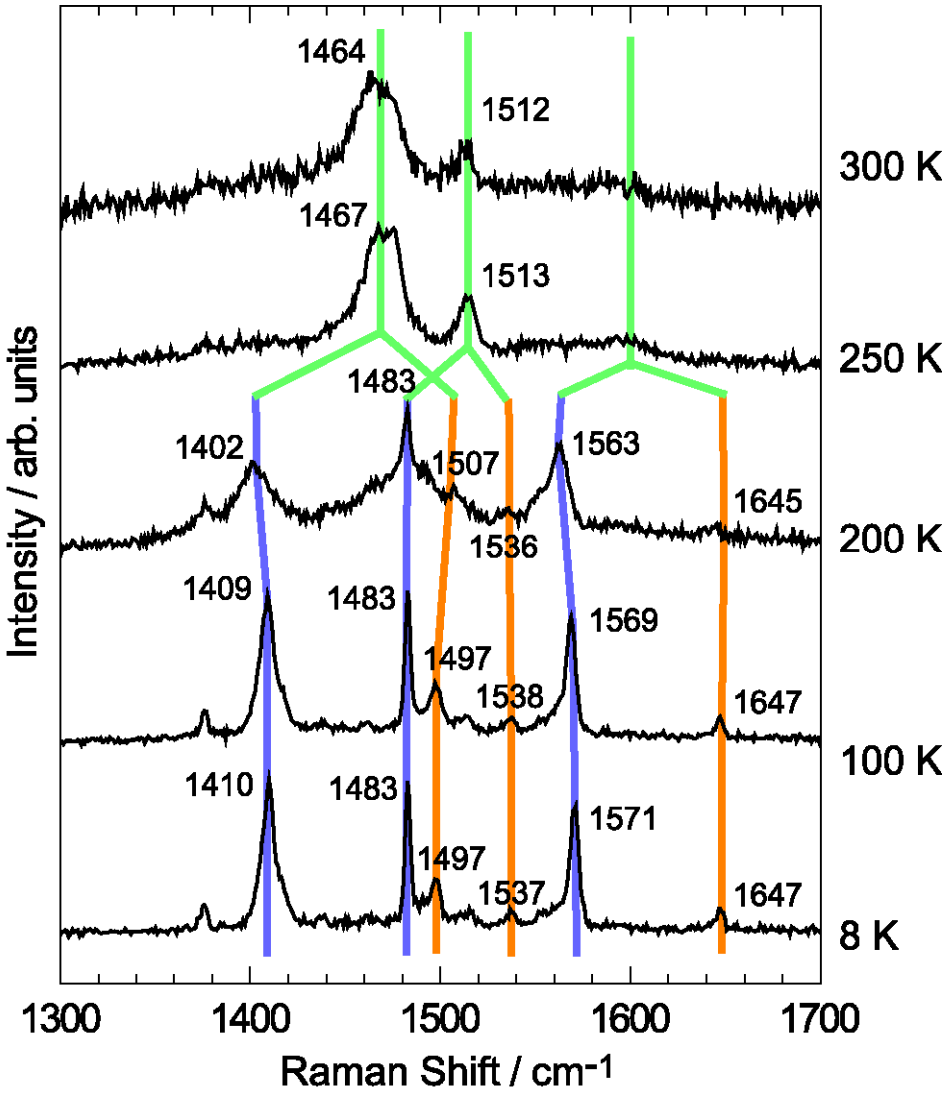

Figure S5. Temperature dependence of Raman spectra of x = 0.13 alloy (batch 4). Bands of EDO-TTF and MeEDO-TTF having a +0.5 charge are indicated by green solid and dotted lines, respectively.

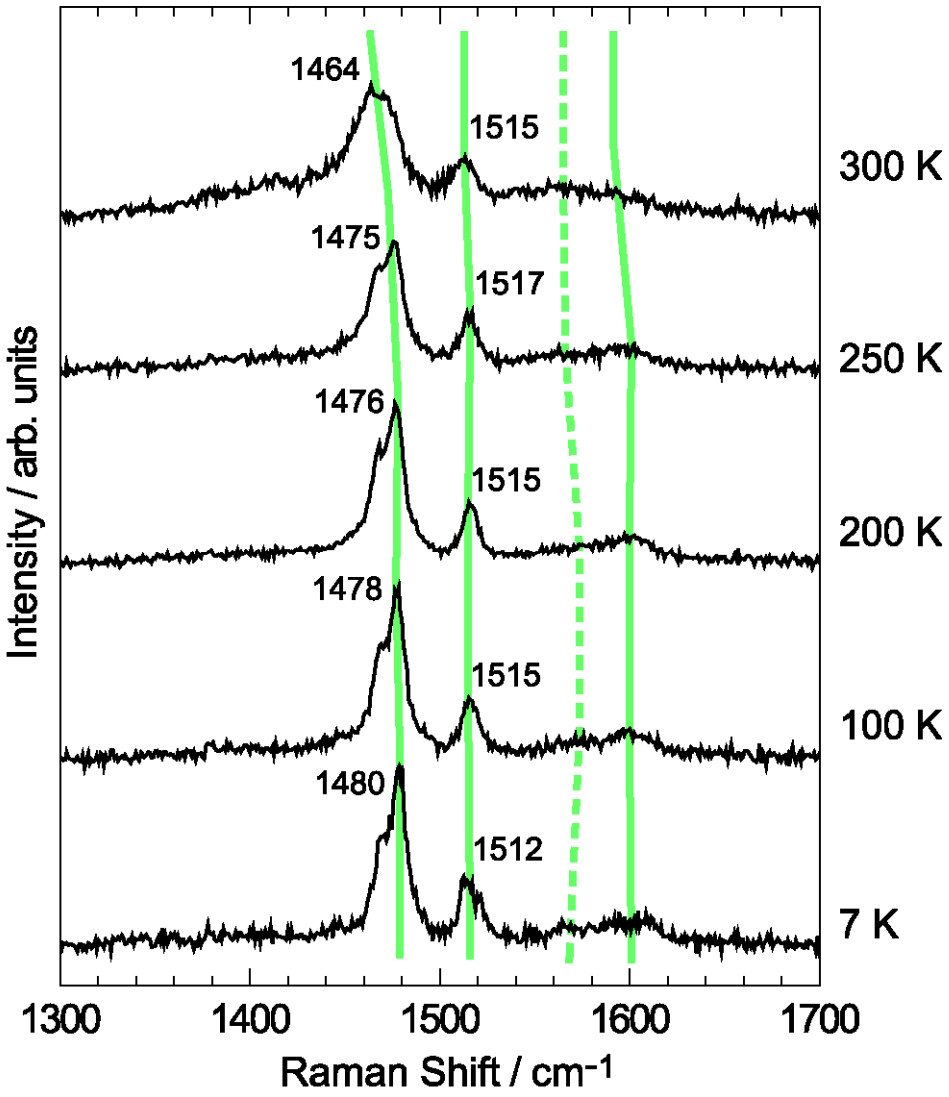

Figure S6. Temperature dependence of Raman spectra of x = 0.52–0.54 alloy (batch 9). Bands of EDO-TTF and MeEDO-TTF having a +0.5 charge are indicated by green solid and dotted lines, respectively.

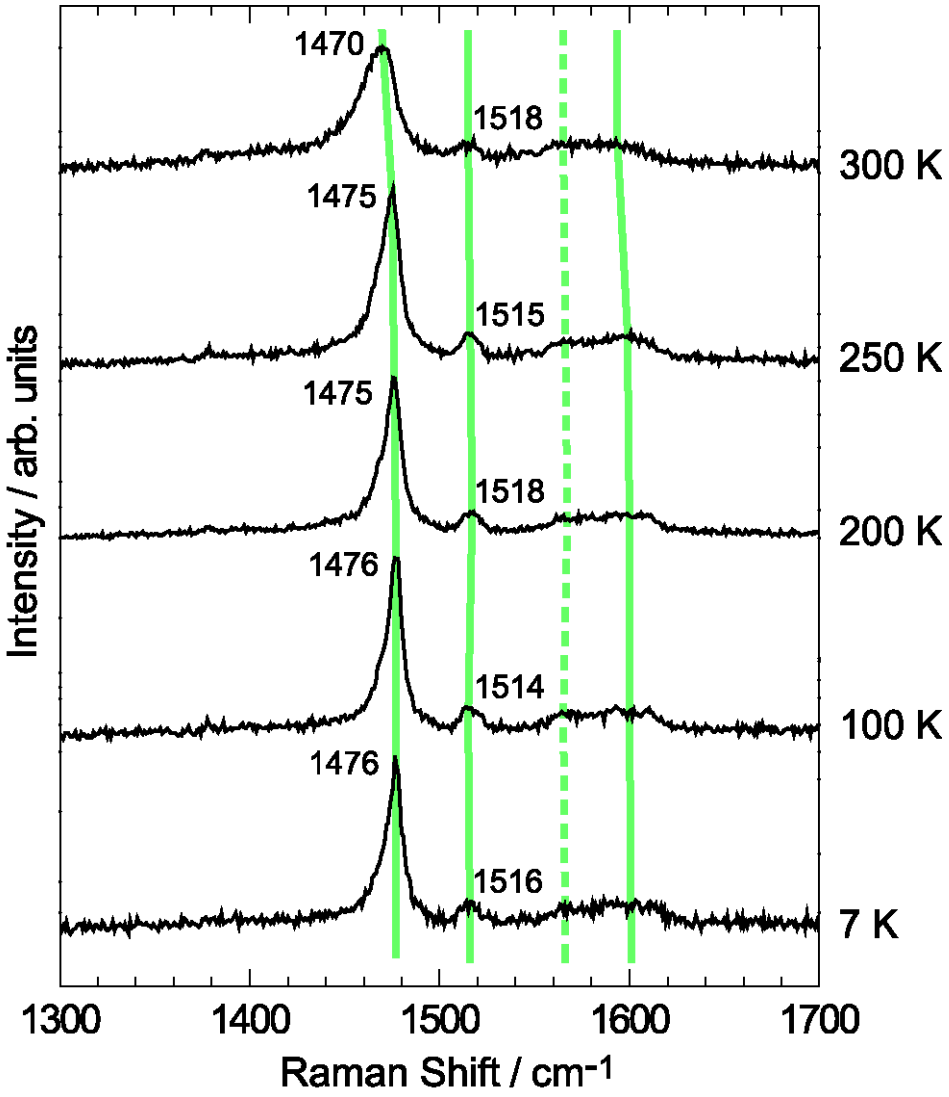

Figure S7. Temperature dependence of activation energy of MeEDO-TTF rich alloys ($x \geq 0.91$, batches 10–12 and pristine $(MeEDO\text{-}TTF)_2PF_6$ ($x = 1$).[ref.17] All the data plotted were taken in the cooling process.